Nano-vaccine that activates the NLRP3 Inflammasome Enhances Tumor Specific Activation of Anti-Cancer Immunity

Saikat Manna,[‡,1,and] Sampa Maiti, [‡,2,α] Jingjing Shen,[1] Adam Weiss,[1,3] Elizabeth Mulder,[1] Wenjun Du,[2] Aaron P. Esser-Kahn[,1]*

1: Pritzker School of Molecular Engineering, University of Chicago, 5640 S. Ellis Ave., Chicago, IL 60637, USA

2: Department of Chemistry and Biochemistry, Science of Advanced Material, Central Michigan University, Mount Pleasant, Michigan 48858, United States.,

3: Department of Chemistry, University of Chicago, 5735 S Ellis Ave., Chicago, IL 60637, USA

and: Current Address: GreenLight Biosciences, Inc.

α: Current Address: Sanofi U.S.

‡: These authors contributed equally.

*: Corresponding author E-mail: aesserkahn@uchicago.edu

KEYWORDS

Nanovaccine, Biomaterials, Adjuvant, Inflammasome, Neoantigen therapy

Table of Contents

Supplementary Methods:

Mass Spectrometry. Electrospray ionization mass spectrometry (ESI-MS) was conducted using a Waters LCT Premier™ XE system. Matrix-assisted laser desorption/ionization mass spectrometry (MALDI-MS) was conducted using a Bruker Ultraflextreme MALDI-TOF-TOF system using Super DHB (Supelco) as a solid support matrix.

Nuclear Magnetic Resonance Spectroscopy. Proton nuclear magnetic resonance (^{1}H-NMR) spectra were recorded at 300 MHz on a Varian Mercury 300 or 500 MHz on a Varian Inova 500 spectrometer or a Bruker 500 spectrometer, with tetramethylsilane (TMS) proton signal as the standard. 13C NMR spectra were recorded at 126 MHz on a Varian Inova 500 spectrometer, with tetramethylsilane (TMS) carbon signal as the standard.

Gel Permeation Chromatography. Gel permeation chromatography (GPC) analyses were conducted using a Viscotek GPC system equipped with a VE 3580 RI detector, VE 112 solvent delivery system, and a column system comprised of one PAS102 and one PAS103 column (Polyanalytik Inc.). The system was equilibrated at 35 °C in DMF, which served as the polymer solvent and eluent with a flow rate of 1.0 mL min^{-1}. Polymer solutions were prepared at a known concentration (ca. 6 mg/mL) and an injection volume of 100 µL was used. Data collection and analyses were performed by OmniSEC software system from Malvern Inc. The GPC system was calibrated using polystyrene standards having molecular weights of 2.5 5.0, 9.0, 17.0 and 50.0 kDa and PDI of 1.05-1.07 (Supelco Analytical, Bellefonte, PA, USA).

Transmission Electron Microscope. Transmission Electron Microscopy (TEM) measurements were performed using a FEI Tecnai F30 300 kV FEG(s) TEM microscope. Carbon-coated copper grids were treated with oxygen plasma before deposition of the samples. The

samples were deposited on the carbon grids for 1 min, and excess samples were wicked away. The samples were allowed to dry under ambient conditions. Samples were stained with uranyl acetate.

Dynamic Light Scattering. Dynamic light scattering (DLS) measurements were performed by a Wyatt Mobius DLS instrument. Measurements were performed at 25^{o}C using a laser wavelength of 532 nm. Scattered light was collected at a fixed angle of 163.5^{o}

High Performance Liquid Chromatography. High performance liquid chromatography (HPLC) was employed to evaluate the composition of PAIs using an Agilent Infinity 1260 analytical HPLC equipped with a Phonomenex Luna C18 column (5 μm, 100 Å, 150 × 4.6 mm) and a UV-VIS detector. First, Free TAT-P6-GWWWG and 2BXy were injected to determine the elution time and molar absorption coefficient at 280 nm of each component. Then, PAIs were degraded by incubating in 0.1% TFA in 1:1 DMSO:water for 4 h. Following TFA treatment, the degraded PAI solution was injected to the HPLC, and the area under the curve of each component peak was referenced to the standard curves to quantify the presence of TAT-P6-GWWWG and 2BXy in the polymer scaffold.

Solid Phase Peptide Synthesis. Fmoc-solid phase peptide synthesis of TAT-P6-GWWWG and neoantigen peptides was performed using a Liberty Blue peptide synthesizer (CEM) using Rink amide resin (100−200 mesh) as the solid support. For the synthesis of TAT-P6-GWWWG, the N-terminus was capped with azidohexanoic acid to allow conjugation to the alkyne-containing SPOE scaffold. Double coupling and extended coupling times were used to couple the arginines and the hexaethylene glycol linker. Peptides were deprotected using a mixture of 85% TFA mixed with 5% water, 5% anisole, and 5% thioanisole. Following deprotection, the crude peptide was precipitated in cold diethyl ether. The crude peptide was then purified using a Phonomenex Luna C18 column (5 μm, 100 Å, 150 × 21.2 mm) on a Gilson preparative HPLC

using a gradient of acetonitrile (containing 0.1% TFA) in water (containing 0.1% TFA) over a period of 15 min at a flow rate of 21.2 mL/ min. The purified peptides were lyophilized and characterized using MALDI-MS.

Synthesis of 2BXy-Azide. The synthesis of compound **2a** was performed based on previously reported synthetic protocol.[S1] Compound **2a** (100 mg, 0.28 mmol) and azidohexanoic acid (48.41 mg, 0.31 mmol) were added in anhydrous DMF following which DIPEA (73.2 µL, 0.42 mmol and HATU (159.70 mg,0.42 mmol) were added to the reaction mixture under argon. The reaction mixture was stirred for 12 h at room temperature following which the solvent was removed under vacuo and the product was purified by silica gel column chromatography using a gradient of 0-5 % methanol in dichromethane, giving compound 2 as a yellow powder (104.8 mg, 0.21 mmol, 75 % yield). ^{1}H NMR (500 MHz, $CDCl_3$) δ 8.52 (s, 1H), 8.22 (d, *J* = 8.3 Hz, 1H), 8.03 (d, *J* = 8.3 Hz, 1H), 7.67 (d, *J* = 8.3 Hz, 1H), 7.44 (t, *J* = 8.3 Hz, 1H), 7.25 (d, *J* = 8.1 Hz, 2H), 7.20 (m, 1H), 6.97 (d, *J* = 8.1 Hz, 2H), 6.21 (s, 1H), 5.75 (s, 2H), 4.41 (d, 2H), 3.75 (m, 2H), 3.22 (t, 2H), 2.87 (t, 2H), 2.22 (m, 2H), 1.86 (s, 2H), 1.80 (m, 2H), 1.65 (m, 2H), 1.56 (m, 2H), 1.42 (m, 2H), 1.38 – 1.33 (m, 2H), 1.26 (s, 1H) 0.93 (t, 3H).ESI-MS: m/z calc'd for $C_{28}H_{34+1}N_8O$: 499.64, observed: 499.65.

Synthesis of 2,3,4-tri-O-acetyl-α-D-glucopyranosyl bromide (SPOE Monomer I). The synthesis of monomer-I was performed based on previously reported synthetic protocol.[S2] Briefly, in a 50 mL disposable polypropylene tube, 2,3,4-tri-*O*-acetyl-6-*O*-*tert*-butyldiphenylsilyl-α-D-glucopyranosyl bromide (1.0 g, 1.65 mmol) was added to anhydrous tetrahydrofuran (7 mL). HF-Py (0.82 g, 70% HF in pyridine, 0.57 g HF, 29 mmol HF) was subsequently added. The reaction was stirred under nitrogen at 4 °C for 12 h. The solvent and excess HF-Py was removed by sparging N_2 gas at 4 °C and the residue was purified by silica gel column chromatography (hexanes/ethyl

acetate = 6/4, R_f = 0.3) to afford the product as a white powder (0.38 g, 62%). ^{1}H NMR (300 MHz, $CDCl_3$) δ 6.64 (d, $J_{1,2}$ = 4.0 Hz, 1H, α-H1), 5.63 (dd, $J_{2,3}$ = 10 Hz, $J_{3,4}$ = 10 Hz, 1H, H-3), 5.14 (dd, $J_{3,4}$ = 10 Hz, $J_{4,5}$ = 10 Hz, 1H, H-4), 4.80 (dd, $J_{2,3}$ = 10 Hz, $J_{1,2}$ = 4.0 Hz, 1H, H-2), 4.09 – 4.06 (m, 1H, H-5), 3.78 (ddd, $J_{6,6'}$ = 13.2 Hz, $J_{6,OH}$ = 8.2 Hz, $J_{5,6}$ = 2.2 Hz, 1H, H-6), 3.63 (ddd, $J_{6,6'}$ = 13.2 Hz, $J_{6',OH}$ = 6.2 Hz, $J_{5,6}$ = 3.5 Hz, 1H, H-6'), 2.29 (dd, $J_{6,OH}$ = 8.2 Hz, , $J_{6',OH}$ = 6.2 Hz, 1H, -OH), 2.10 (s, 3H), 2.09 (s, 3H), 2.05 (s, 3H). ^{13}C NMR (126 MHz, $CDCl_3$) δ 170.80 (C=O), 170.03 (C=O), 170.01 (C=O), 87.07 (α-C1), 74.57 (C-5), 71.04 (C-2), 69.98 (C-3), 67.85 (C-4), 60.53 (C-6), 20.90 (-OAc), 20.88 (-OAc). ESI-MS calc for $C_{12}H_{17}BrNaO_8$ $[M+Na]^+$ = 391.00, 393.00, found: 391.12, 393.13.

Synthesis of 3-propargyl-2,4-di-*O*-acetyl-α-D-glucopyranosyl bromide (SPOE monomer II) The synthesis of monomer II was performed based on previously reported synthetic protocol.[S2] Briefly, in a 50 mL disposable polypropelene tube, 3-propargyl-2,4-di-*O*-acetyl-6-*O*-*tert*-butyldiphenylsilyl -α-D-glucopyranosyl bromide (1.0 g, 1.7 mmol) was added to anhydrous tetrahydrofuran (7.0 mL). HF-Py (0.82 g, 70% HF in pyridine, 0.57 g HF, 29 mmol HF) was subsequently added. The reaction was stirred under nitrogen at 4 °C for 12 h. The solvent and excess HF-Py was removed by sparging N_2 gas at 4 °C and the residue was purified by silica gel column chromatography (hexanes/ethyl acetate = 6/4, R_f = 0.3) to afford the product as a white powder (0.40 g, 66%). ^{1}H NMR (500 MHz, $CDCl_3$) δ 6.64 (d, J = 3.9 Hz, 1H, α-H1), 5.02 (m, 1H, H-4), 4.68 (dd, J = 9.6, 3.9 Hz, 1H, H-2), 4.31 (m, 2H, $-CH_2$), 4.12 (dd, $J_{2,3}$ = 10 Hz, $J_{3,4}$ = 10 Hz, 1H, H-3), 3.96 (m, 1H, H-5), 3.69 (ddd, $J_{6,6'}$ = 13.2 Hz, $J_{6,OH}$ = 8.2 Hz, $J_{5,6}$ = 2.2 Hz, 1H, H-6), 3.58 (ddd, $J_{6,6'}$ = 13.2 Hz, $J_{6',OH}$ = 6.2 Hz, $J_{5,6}$ = 3.5 Hz, 1H, H-6'), 2.49 (t, J = 2.4 Hz, 1H, HC≡C), 2.13 (d, J = 10.0 Hz, 6H),), 2.14 (s, 3H), 2.11 (s, 3H), ^{13}C NMR (126 MHz, $CDCl_3$) δ 170.66 (C=O), 169.27 (C=O), 88.47 (α-C1), 79.54 (acetylene -CH), 76.33 (C-3), 74.77 (C-5), 72.73 (C-

2), 68.69 (C-4),61.08 (O-CH_2), 60.31 (C-6), 20.86 (-OAc). ESI-MS calc for $C_{13}H_{17}BrNaO_7$ $[M+Na]^+$ = 388.17, found: 388.06.

Synthesis of sugar poly(orthoester) (SPOE). The synthesis of functional glucose co-poly(orthoester) (SPOE) was performed based on previously reported synthetic protocol.[S2] To a Schlenk flask was added monomer **I (**0.20 g, 0.54 mmol**),** monomer **II, (**0.05 g, 0.11 mmol), anhydrous CH_2Cl_2 (5 mL), tetrabutylammonium iodide (TBAI) (0.199 g, 0.54 mmol) and *N,N*-diisopropylethylamine (DIPEA, 0.21 g, 1.63 mmol). The reaction mixture was refluxed under argon atmosphere for 20 h. The solvent was removed by reduced pressure. The polymer was precipitated three times using a mixture of water/methanol (9/1, v/v) at 4 ^oC to afford **1** as a white powder (0.18 g, 70%). M_n^{GPC} = 6.3 kDa, PDI =1.3. ^1H NMR (500 MHz, $CDCl_3$) δ = 5.71 (d, *J* = 5.0, 1H, α-H1), 5.13 (m, 1H, H-3), 4.92-4.90 (t, *J* = 9.0, 1H, H-4), 4.42 (s, -CH_2), 4.27 (m, 1H, H-2), 3.80 – 3.78 (m, 1H, H-5), 3.62 – 3.55 (m, 2H, H-6,6'), 2.44 (t, acetylene proton), 2.11 (m, 3H), 2.07 (s, 3H), 1.69 (s, 3H). ^{13}C NMR (126 MHz, CDCl3) 169.99 (C=O), 169.51 (C=O), 121.34 (orthoester C), 97.30 (C1), 80.06 HC≡C), 72.81 (C-2), 70.09 (C-3), 68.35 (C-4), 67.81 (C-5), 63.25 (C-6), 21.12 (-OAc), 20.68 (-OAc), 20.59 (-CH_3).

Analysis of encapsulation efficacy of neoantigen peptides. PAI (750 μg) was incubated to 200 μg of each peptide in a total volume of 1 mL DI water. The solution was then centrifuged at 5000 x g to precipitate out the particles. The supernatant was then injected to an Agilent Infinity 1260 analytical HPLC equipped with a Phonomenex Luna C18 column (5 μm, 100 Å, 150 × 4.6 mm) and a UV-VIS detector set to 280 nm, and the free peptide in solution was quantified by HPLC analysis relative to dissolved peptide standards.

Table of Antibodies Used

Antibody	Fluorophore	Clone	Experiment	Vendor
CD16/32	N/A	93	Multiple studies	BioLegend
SIINFEKL:H2K^{b}	PE	25-D1.16	Ag presentation	BioLegend
Zombie NIR	N/A	N/A	Multiple studies	BioLegend
CD3	PE	17A2	T cell ICS	BioLegend
CD4	APC	RM4-5	T cell ICS	BioLegend
CD8	APC	53-6.7	T cell ICS	BioLegend
IFN-gamma	AF488	XMG1.2	T cell ICS	BioLegend
PD-L1	N/A	10F.9G2	Checkpoint blockade	Bio X Cell
CTLA4	N/A	9D9	Checkpoint blockade	Bio X Cell
FOXP3	N/A	FJK-163	Immunohistochem	eBioscience
CD4	N/A	5SM95	Immunohistochem	eBioscience
CD8	N/A	4SM15	Immunohistochem	eBioscience

Supplemental Synthetic Schemes

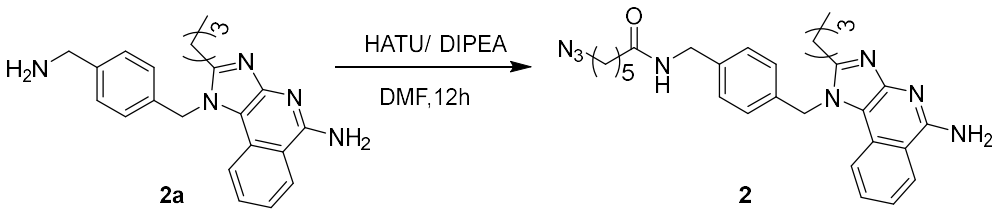

Scheme 1: The synthesis of azide functionalized toll like receptor (7/8) agonist (2BXy-azide) used to prepare the PAI.

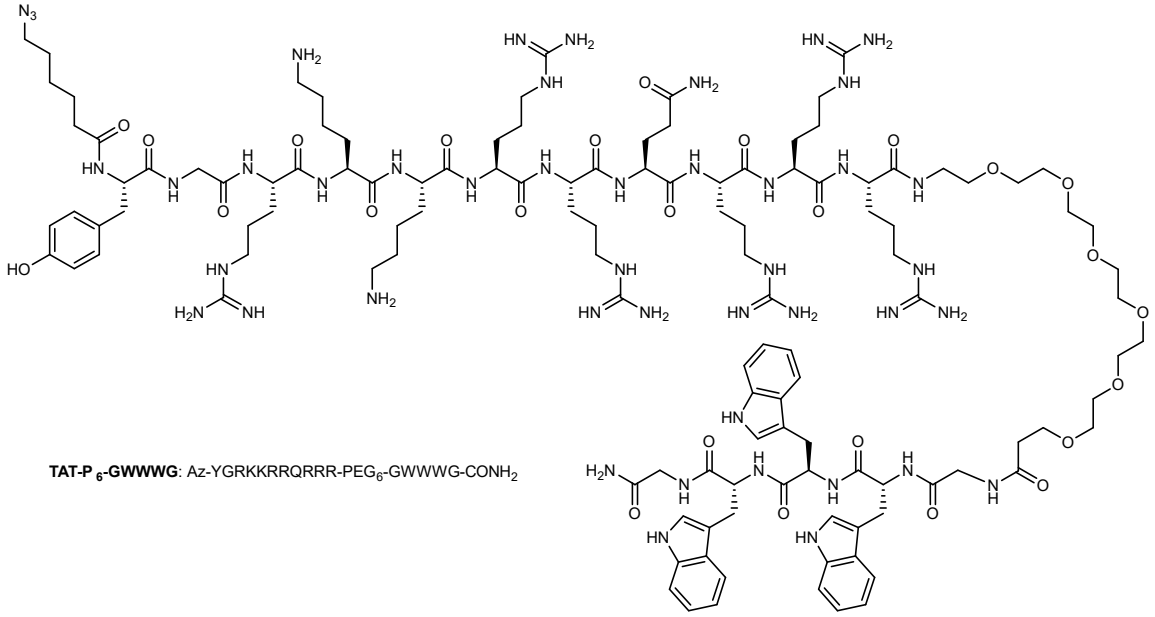

Scheme 2: Chemical structure of the azide modified TAT-P6-GWWWG peptide used to prepare PAI.

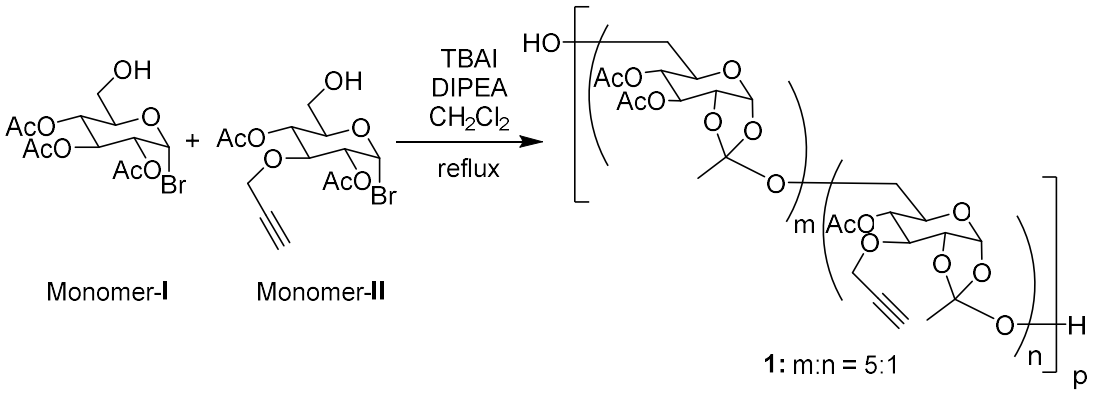

Scheme 3: The synthesis of sugar poly(orthoester) (SPOE) scaffold **1**.

Supplemental Results

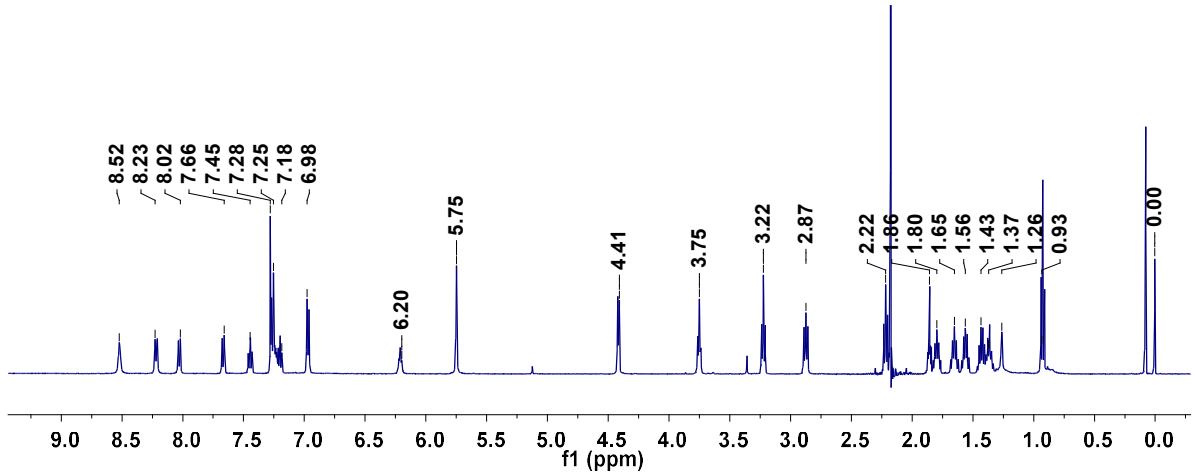

Figure S1: ^{1}H-NMR spectrum of 2BXy azide **(2)**

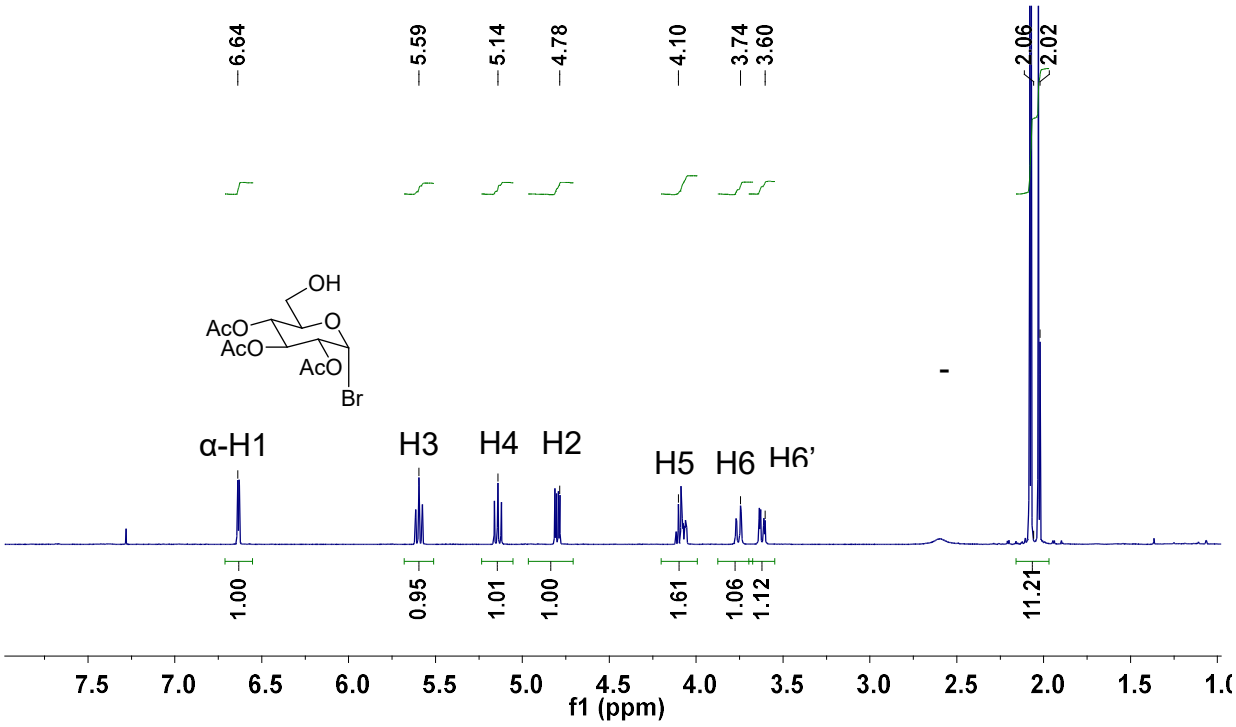

Figure S2 ^{1}H-NMR spectrum of SPOE monomer I.

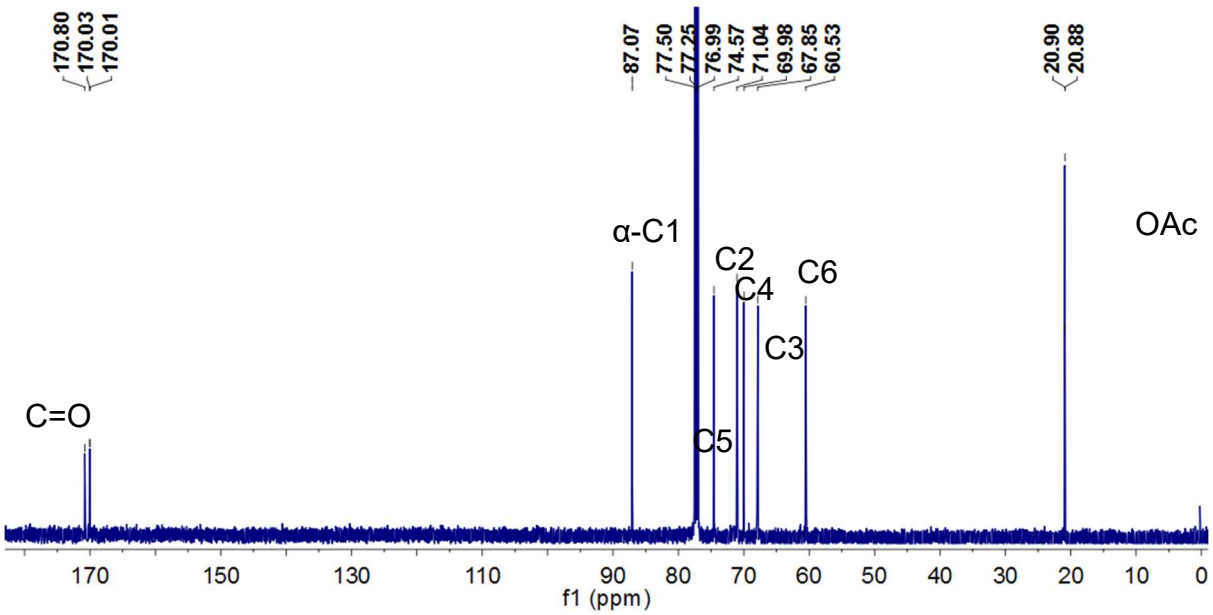

Figure S3: ^{13}C-NMR spectrum of SPOE monomer I

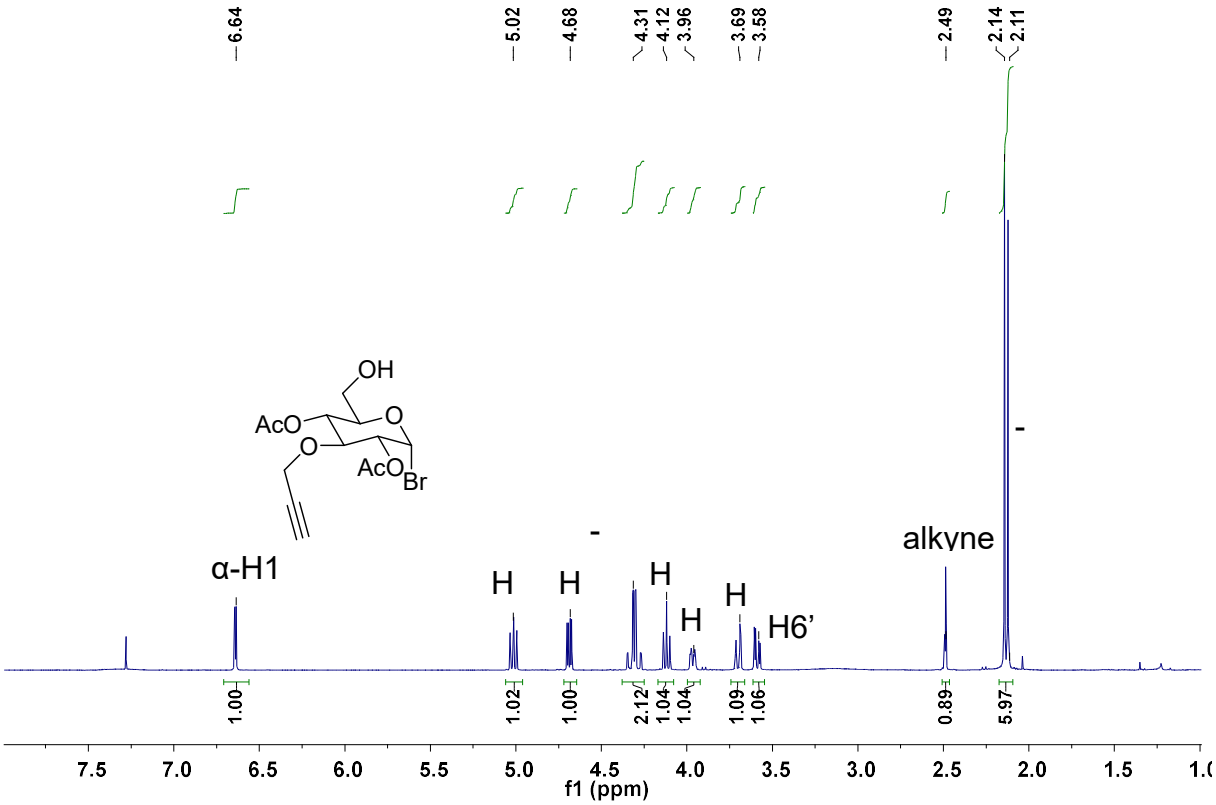

Figure S4. [1]H-NMR spectrum of SPOE monomer **II**

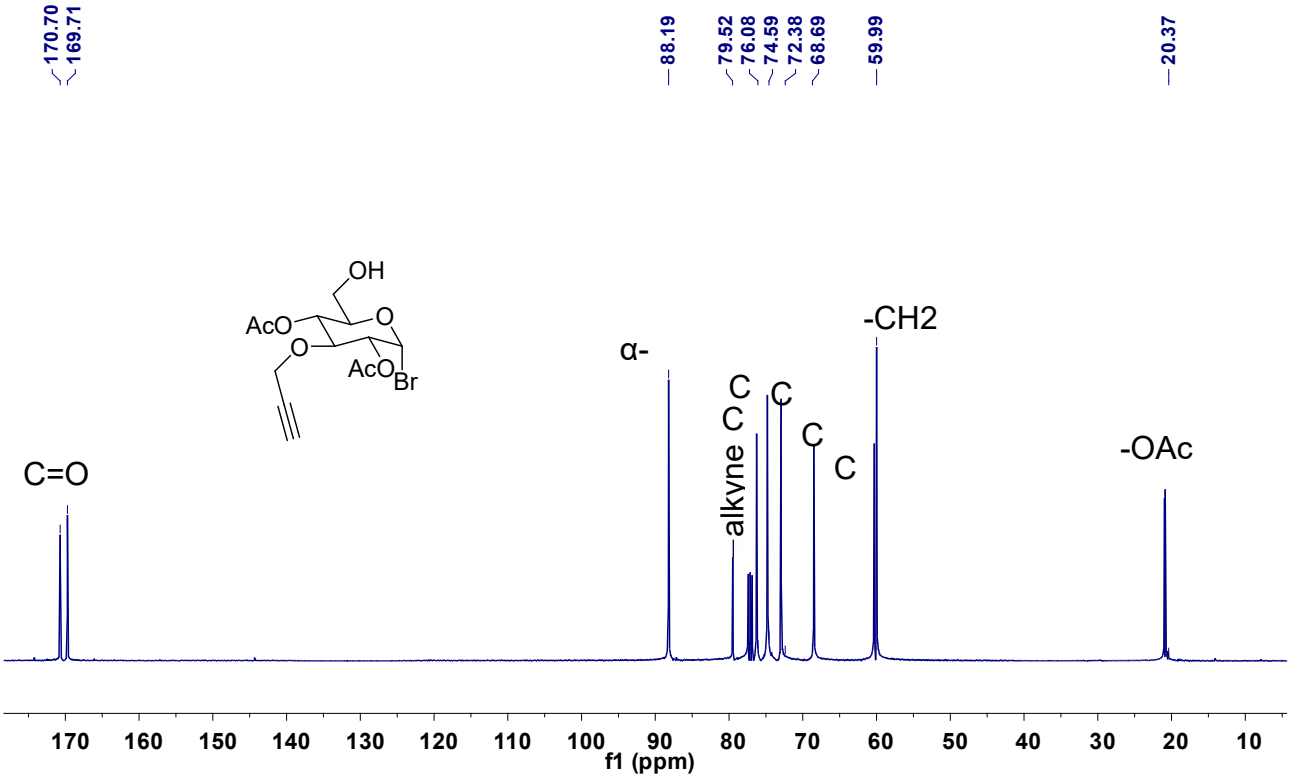

Figure S5. ^{13}C-NMR spectrum of SPOE monomer **II**

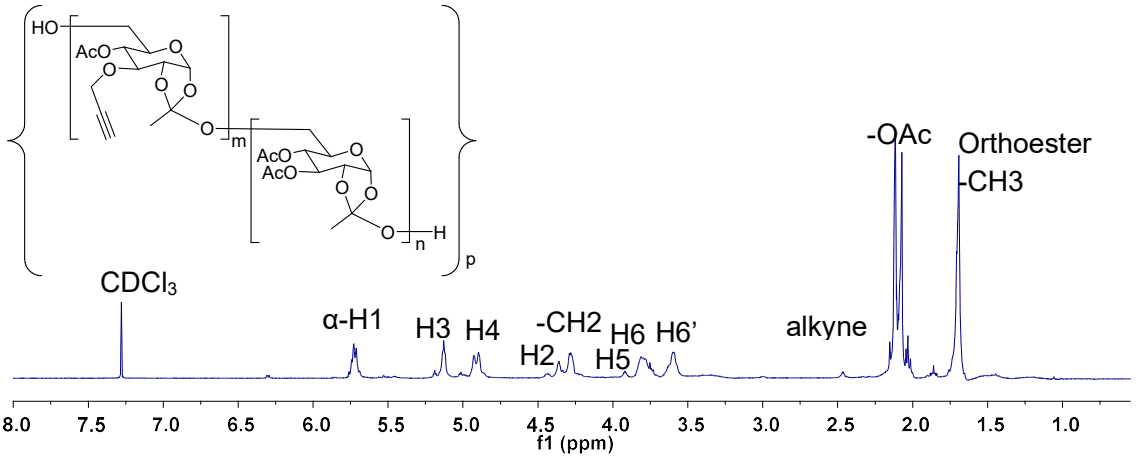

Figure S6. ^{1}H-NMR spectrum of SPOE polymer

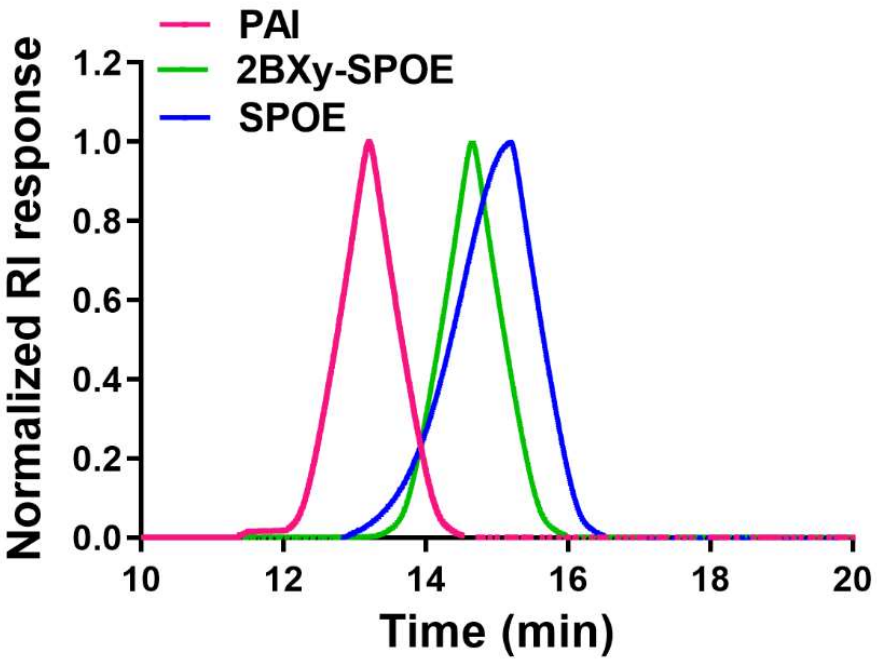

Figure S7. GPC analysis of SPOE, 2BXy-SPOE and PAI

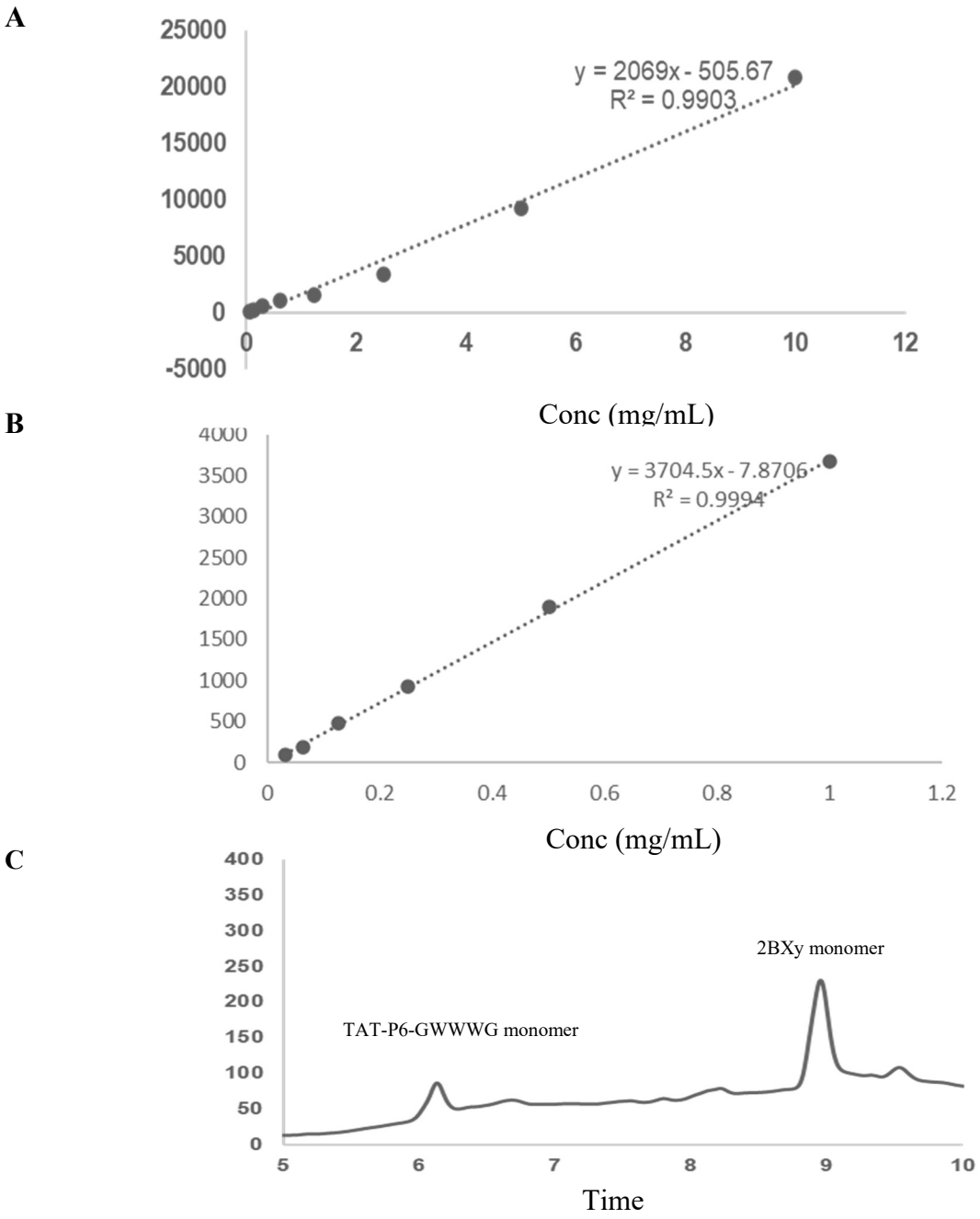

Figure S8: HPLC analysis of PAI. PAI was degraded by incubating in 0.1% TFA in 1:1 DMSO:water for 4 h. Following this, the solution was injected in a C8 column on an Agilent analytical HPLC and monitored at 280 nm using the UV-vis detector. Two peaks were observed (C) and confirmed as TAT-P6-GWWWG-glucose and 2BXy-glucose by ESI-MS. The concentration of TAT-P6-GWWWG peptide and 2Bxy in the polymer were determined by analysis of peak integration (C) based on standard curves for TAT-P6-GWWWG (A) and 2BXy (B).

Entry	Theoretical calculation			Experimental quantification		
	Ratios	TLR7/8a	TATGWWWG	TLR 7/8a	TATGWWWG	Ratios
1	(0.5:1)	1	2	0.8	1.8	(0.44:1)
2	(1:1)	2	2	2.1	1.8	(1.2:1)
3	(1.5:1)	3	2	2.7	1.8	(1.5:1)
4	(2:1)	4	2	3.9	1.8	(2.2:1)

Table S1. Ratio of TAT7/8 and TAT-P6-GWWWG in polymer library as determined by HPLC.

A **B**

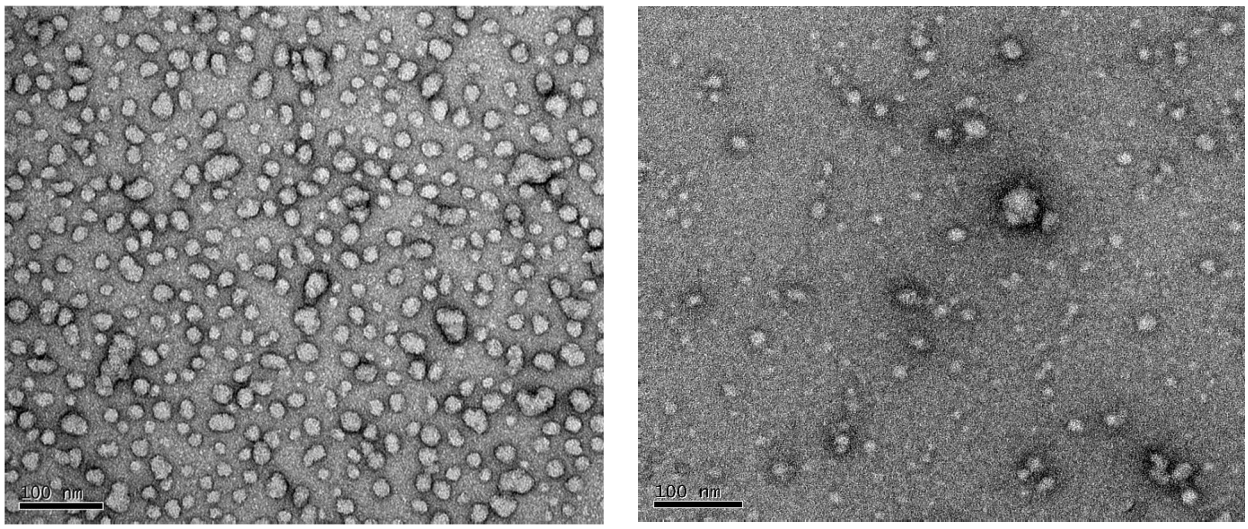

Figure S9. TEM images of (A) PAI with 1.5:1 ratio of 2BXy:TAT-P6-GWWWG and (B) 0:1 ratio of 2BXy:TAT-P6-GWWWG (formulation control).

Entry	Ratio (TLR7/8a : Tat-GWWWG	Diameter (TEM) nm	Hydrodynamic Radius (DLS) nm
1	0:1	15.2 ± 4.3	48.2 ± 3.9
2	0.5:1	16.9 ± 3.1	54.6 ± 4.9
3	1:1	18.2 ± 3.4	63.2 ± 5.7
4	1.5:1	23.1 ± 3.9	72.4 ± 6.2
5	2:1	32.2 ± 5.8	84.1 ± 8.3

Table S2. Size characterization of PAI library

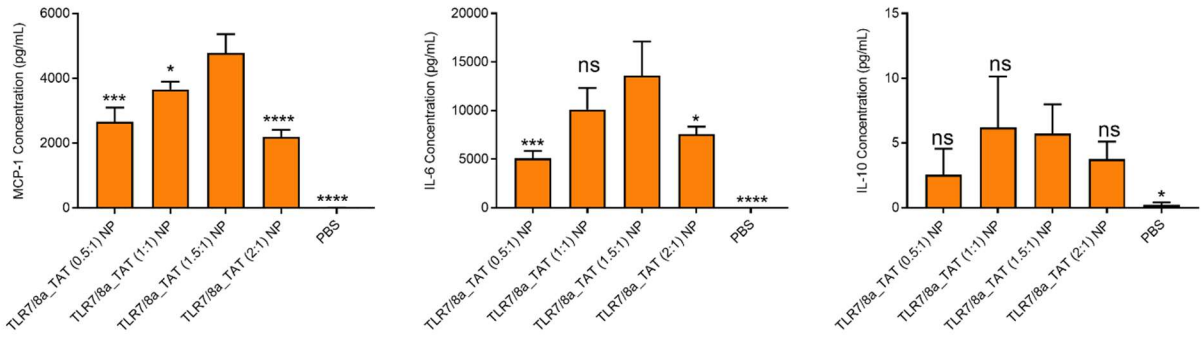

Figure S10. Additional non-significant cytokine data determined from multiplexed bead analysis used in **Figure 1C**. Statistical significance was determined using one-way ANOVA with Dunnett's multiple comparisons test.

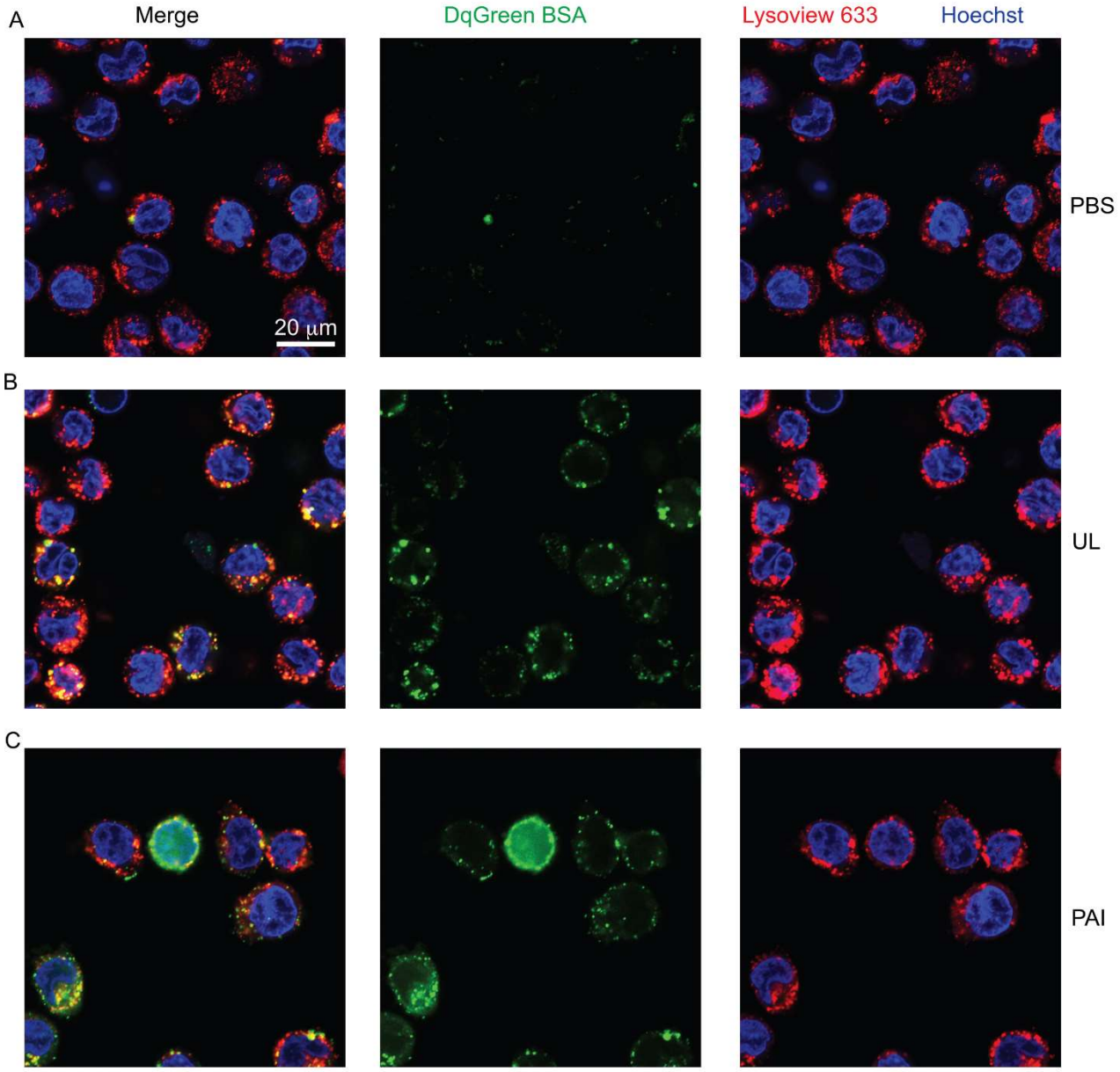

Figure S11. PAI induces endosomolysis and cytosolic delivery. Various activators were incubated along with DQ Green BSA on THP-1 cells for 12 h and cells were stained with Hoechst and Lysoview 633 followed by confocal microcopy imaging. Representative images for (A) PBS, (B) Unlinked mixture, and (C) PAI.

Peptide	Sequence	Isoelectric Point (pI)
M30	PSKPSFQEFVDWENVSPELNSTDQPFL	3.79
M48	SHCHWNDLAVIPAGVVHNWDFEPRKVS-EE	5.79
M27	REGVELCPGNKYEMRRHGTTHSLVIHD	5.82

Table S3. List of B16-F10 neoantigen peptides synthesized for immunotherapy studies. The neoantigens were identified from reference S3.

A

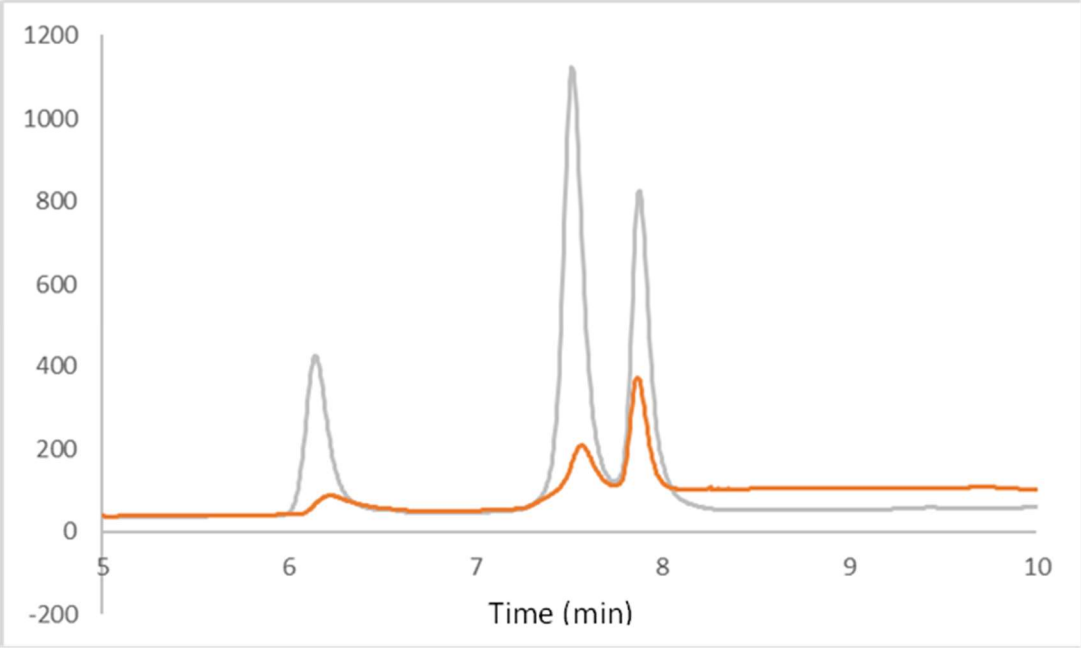

B

Peptide	Encapsulation Efficiency
M27	82
M48	81
M30	64

Figure S12. (A) Representative HPLC analysis of antigen cocktail (gray) and un-encapsulated B16.F10 antigen from PAI-antigen formulation (orange). (B) Using this analysis, the encapsulation efficiency of B16.F10 peptides was determined.

Peptide	Sequence	Isoelectric Point (pI)
M03	DKPLRRNNSYTSYIMAICGMPLDSFRA-EEE	6.42
M20	PLLPFYPPDEALEIGLELNSSALPPTE-KK	4.25
M90	LHSGQNHLKEMAISVLEARACAAAGQS-EE	6.07
GP70	SPSYAYHQF-EE	5.26

Table S4. List of CT26 neoantigen peptides synthesized for immunotherapy studies. The neoantigens were identified from reference S4.

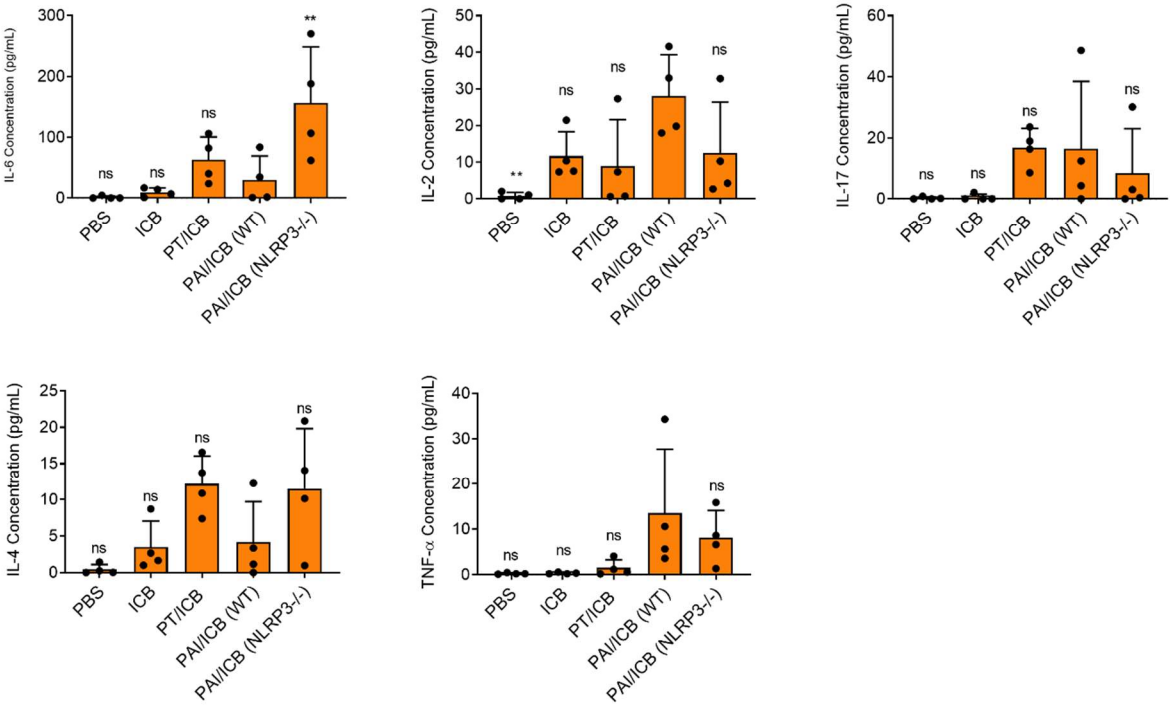

Figure S13. Additional non-significant cytokine data determined from multiplexed bead analysis used in **Figure 4**. Statistical significance is noted relative to PAI/ICB (WT) using one-way ANOVA with Dunnett's multiple comparisons test.

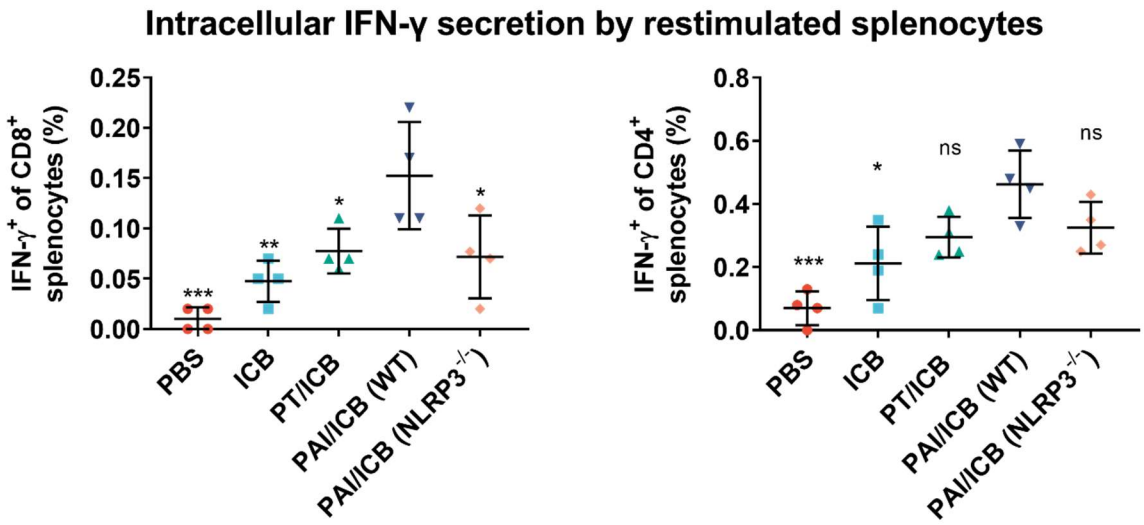

Figure S14. Splenocytes were stimulated ex-vivo with neoantigen peptide cocktail for 48 h, then fixed, permeabilized, stained for IFN-γ and T cell lineage markers, and analyzed *via* flow cytometry. Statistical analyses were performed using one-way ANOVA with Dunnett's multiple comparisons test (determined relative to PAI/ICB WT treatment.)

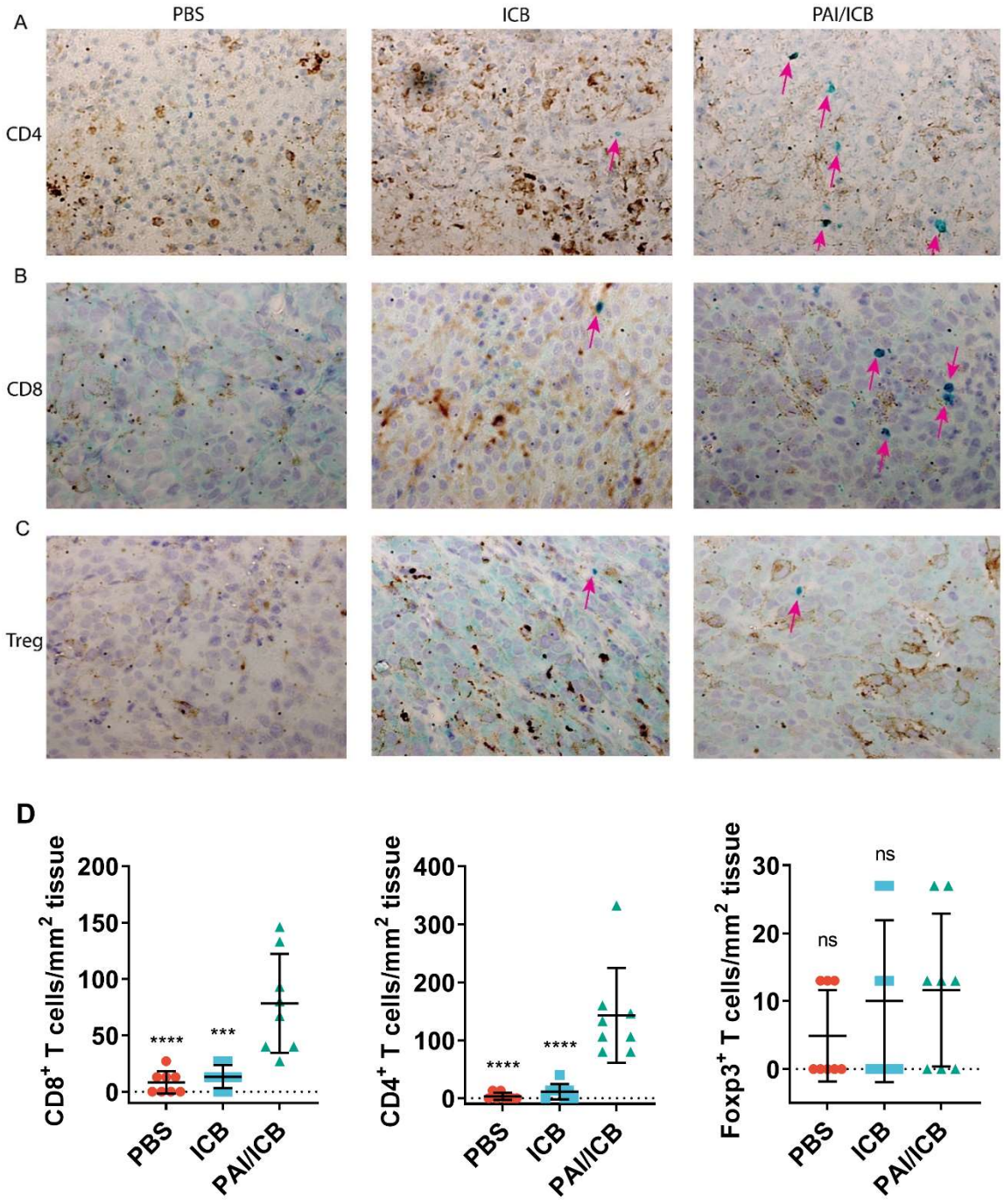

Figure S15. Immunohistochemical (IHC) analysis of tumor tissues. (A-C) Representative IHC staining of tumor tissues from PBS, ICB and PAI groups on day 22. Tumor infiltrating T-cells (CD4, CD8 and Foxp3) are stained in green and indicated with arrows. (A) CD4, (B) CD8, and (C) Foxp3 staining. (D) Quantitative summary data from 8 IHC samples per group. Statistical significance is determined relative to PAI/ICB using one-way ANOVA with Dunnett's multiple comparisons test.

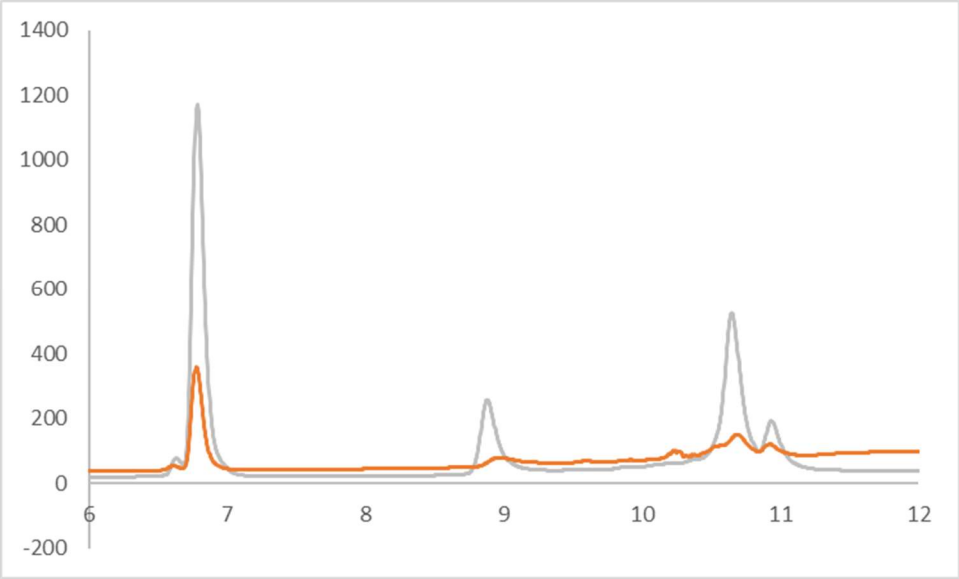

Peptide	Encapsulation Efficiency (%)
GP70	73
M90	82
M03	84
M20	76

Figure S16. (A) Representative HPLC analysis of antigen cocktail (gray) and un-encapsulated CT26 antigen from PAI-antigen formulation (orange). (B) Using this analysis, the encapsulation efficiency of CT26 peptides was determined.

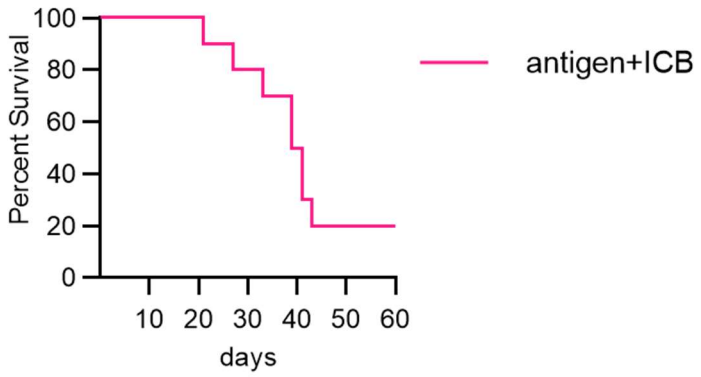

Figure S17: Kaplan-Maier survival curve of antigen+ICB treated mice in CT-26 model. This experiment was conducted in parallel with Figure 5B and demonstrates no statistical difference between antigen+ICB and ICB alone.

Supplementary References

(S1) Manna, S.; Maiti, S.; Shen, J.; Du, W.; Esser-Kahn, A. P. Pathogen-like Nanoassemblies of Covalently Linked TLR Agonists Enhance CD8 and NK Cell-Mediated Antitumor Immunity. *ACS Cent Sci* **2020**, *6* (11), 2071-2078.

(S2) Maiti, S.; Manna, S.; Shen, J.; Esser-Kahn, A. P.; Du, W. Mitigation of hydrophobicity-induced immunotoxicity by sugar poly (orthoesters). *J Am Chem Soc* **2019**, *141* (11), 4510-4514.

(S3) Kreiter, S.; Vormehr, M.; van de Roemer, N.; Diken, M.; Lower, M.; Diekmann, J.; Boegel, S.; Schrors, B.; Vascotto, F.; Castle, J. C.; Tadmor, A. D.; Schoenberger, S. P.; Huber, C.; Tureci, O.; Sahin, U., Mutant MHC class II epitopes drive therapeutic immune responses to cancer. *Nature* **2015**, *520* (7549), 692-696.

(S4) Li, A. W.; Sobral, M. C.; Badrinath, S.; Choi, Y.; Graveline, A.; Stafford, A. G.; Weaver, J. C.; Dellacherie, M. O.; Shih, T. Y.; Ali, O. A.; Kim, J.; Wucherpfennig, K. W.; Mooney, D. J., A facile approach to enhance antigen response for personalized cancer vaccination. *Nat Mater* **2018**, *17* (6), 528-534.